E 21
FERMILAB-CONF-77-126-E

CALT 68-626
ENERGY RESEARCH AND
DEVELOPMENT REPORT

TOTAL CROSS-SECTIONS AND MEAN Y FROM CHARGED CURRENT ν_μ AND $\bar{\nu}_\mu$ COLLISIONS*

(CITFR Experiment)

B. C. Barish, J. F. Bartlett, A. Bodek†, K. W. Brown
D. Buchholz††, Y. K. Chu, F. Sciulli, E. Siskind,
and L. Stutte§,
California Institute of Technology, Pasadena, California 91125

and

H. E. Fisk, G. Krafczyk, and D. Nease
Fermi National Accelerator Lab, Batavia, Illinois 60510

and

O. Fackler

Rockefeller University, New York, New York 10021

(Talk presented by F. Sciulli at 1977 International Symposium on Lepton and Photon Interactions at High Energies, August 25-31, 1977 in Hamburg, Germany.)

ABSTRACT

New normalized data on ν_μ and $\bar{\nu}_\mu$ interactions, from the Caltech-Fermilab-Rockefeller experiment, are presented. Measurements of small y cross-sections, $\frac{1}{E}\frac{d\sigma}{dy}\Big|_{y=0}$, of total cross-sections σ/E, and of mean y, $\langle y \rangle$, are presented for a set of discrete neutrino energies, E, covering the range $45<E<205$ GeV.

---

* Work supported by the U.S. Energy Research and Development Administration. Prepared under Contract EY-76-C03-0068 for the San Francisco Operations Office.

† Present Address: University of Rochester, Rochester, New York 14627

†† Present Address: Northwestern University, Evanston, Illinois 60201

§ Present Address: Fermi National Accelerator Lab, Batavia, Illinois 60510

CONTENT

I. Introduction

II. The E-21 Experiment

A. Directly Measured Flux.
B. Calibration of Muon and Hadron Energies.
C. Separation of ν_π and ν_K Events.
D. Azimuthal Acceptance Corrections (MT events): Small y Cross-sections.
E. Azimuthal Acceptance Corrections (HT events): Large y Cross-sections.
F. Corrections for Polar Angle Losses (θ_μ > 360 mrad).

III. Total Cross-sections and Mean y.

A. Comparisons with GIM and Asymptotic Freedom.
B. The b-Quark Hypothesis.
C. Comparisons with HPWF Data.
D. The Question of Energy Dependence.

IV. Integrated Structure Functions.

A. Checking the Validity of Equation (1).
B. Structure Functions Versus Energy.

V. Conclusions

I. INTRODUCTION

The topic of charged currents requires a short introduction to define the associated parameters. Within the usual framework, one writes the following equation:[1]

$$\frac{d\sigma^{\nu,\bar{\nu}}}{dy} = \frac{G^2ME}{\pi}\left\{(1-y)f_2 + \frac{y^2}{2}f_1 \pm y(1-\frac{y}{2})f_3\right\} \qquad (1)$$

in terms of the three integrated structure functions: $f_1 = \int 2xF_1(x)dx$, $f_2 = \int F_2(x)dx$, and $f_3 = \int xF_3(x)dx$. The primary assumptions contained in this equation are scaling, charge symmetry, and V-A. The Callan-Gross relation for spin 1/2 objects would, in addition, imply that $f_1 = f_2$. The B-parameter, made famous by Myatt and Perkins,[2] is defined as $B \equiv f_3/f_2$. If the Callan-Gross relation is assumed, there are only two integrated parameters: f_2, and B or f_3.

After introducing the parameters, it is incumbent upon the speaker to give a short history of the subject. Allow me to shorten the recent history by summarizing it with the graph shown in Fig. 1: the B parameter as a function of neutrino energy. With the assumption of scaling, B should be independent of energy.

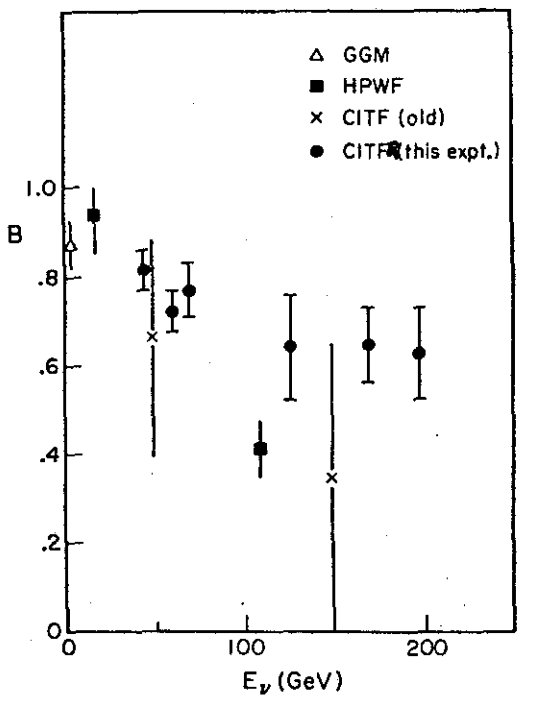

Fig. 1 $B = f_3/f_2$ from older experiments (ref. 3, 4, 5) compared with the results of this experiment.

In this field, one usually starts with that which existed in the beginning: the Gargamelle data.[3] Their point at $E \sim 5$ GeV is all that existed on the first day. On the second day, the HPWF data[4] came to pass and it seemed to indicate a rather dramatic change in B

as a function of neutrino energy. On the third day, there came to pass the Caltech-Fermilab (CITF) experiment,[5] published about 1-1/2 years ago on measurements of the y-distribution from antineutrinos. It wasn't much help in resolving the question, due to very large errors. Older measurements by this group of normalized total cross-sections[6] would give B values considerably higher, but again with errors too large to be conclusive. There were also some later bubble chamber data on y-distribution shapes from Fermilab,[7] which lay in the lower part of this energy region; these indicated some energy dependence, but again the errors were large. On the basis of the average of the two older CITF points shown,[6] we concluded that there was some indication of differences in the shapes of y-distributions at high energies (CITF) compared to low energies (GGM).

The new CITFR data I am going to present today will result in the six B-values shown. The remainder of my talk involves the more accurate experiment[8-12] (E21) that resulted in these new values, followed by a discussion of the data itself. The experiment obtained both total normalized cross sections and shape information (i.e. mean y) from a sample which covers almost the entire phase space. Some simple checks of the validity of equation (1) with regard to the data will also be presented.

II. THE E-21 EXPERIMENT

The E-21 experiment contains roughly 30,000 events, of which a little over 1/3 are antineutrino events. There were three settings of the dichromatic beam for ν_μ and three for $\bar{\nu}_\mu$, giving six spectra for ν_μ and six for $\bar{\nu}_\mu$. The analysis of the total cross-section and mean y has been finished, so the numbers you will see have all the stated corrections applied, and all the systematic effects are included in the error analysis.

The technique involved use of the Fermilab narrow-band beam as in the previous experiment. There are some substantial differences, though, between the cross-section measurement I will describe today and the previous measurements[6] by this same group. (The quoted errors are smaller by about a factor of five.) Indeed, much of the last five or six years has been spent in learning how to do this experiment correctly. I would like to point out some unique and novel features which give us assurance that the answers are correct.

A. Directly Measured Flux

Neutrino fluxes are obtained from intensity measurements of the momentum analyzed pions and kaons, some of which decay into the beam neutrinos. The total charged particle intensity was continuously monitored with several devices whose linearity was established to be better than 1% in the region of interest. The calibration of intensity was done by two separate methods that agreed with each other to 2%. The particle ratios, which are required to give the separate pion and kaon neutrino fluxes, were measured with a Cherenkov counter. A Cherenkov measurement is shown in Fig. 2 for the highest energy antineutrino setting, at which the K^-/π^- ratio is smallest. The background curve drawn under the K^- signal is not calculated; it is measured. This could be done because counting techniques were employed which utilized a second $\hat{C}$ counter, electron and

muon identifiers. After studying and analyzing the data at all of the beam settings in some detail, we have assigned neutrino flux errors of 5-9%, depending on the flux type and beam setting, and an additional overall calibration error of 4%.

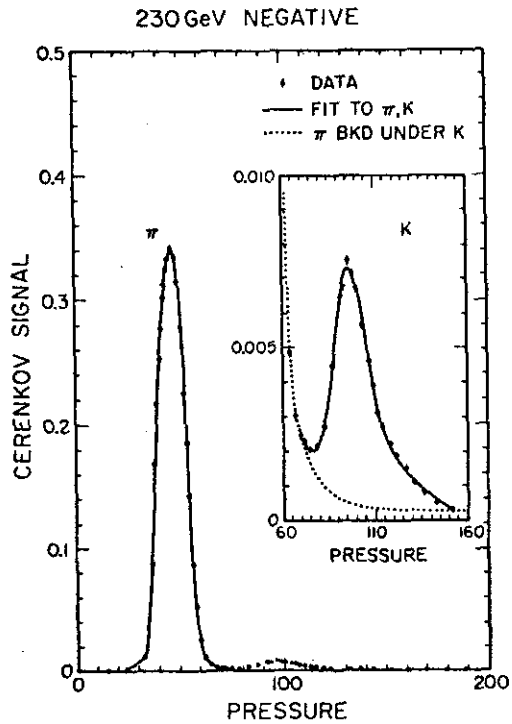

Fig. 2. Cherenkov curve for measurement of the K^-/π^- ratio at the highest energy setting, where this ratio is lowest. The signal/noise at the K^- peak (see inset) is about 7/1. The dotted background curve under the K^- was simultaneously measured.

B. Calibration of Muon and Hadron Energy

The events collected by the apparatus contain final states with both a muon and hadrons. It is very important, especially when one talks about quantities like <y> (i.e. the ratio of mean hadron energy to neutrino energy), that the calibration of muon and hadron energy be self-consistent with the neutrino beam energy. This internal check was performed at all of the six beam settings for the pion and kaon neutrinos separately (i.e., 12 mean neutrino energies). The internal calibration was self-consistent to a typical accuracy of 4%. This agrees with our estimate of the gain stability for the calorimeter. Therefore, a 4% contribution has been included in the systematic error assigned to our quoted <y> values.

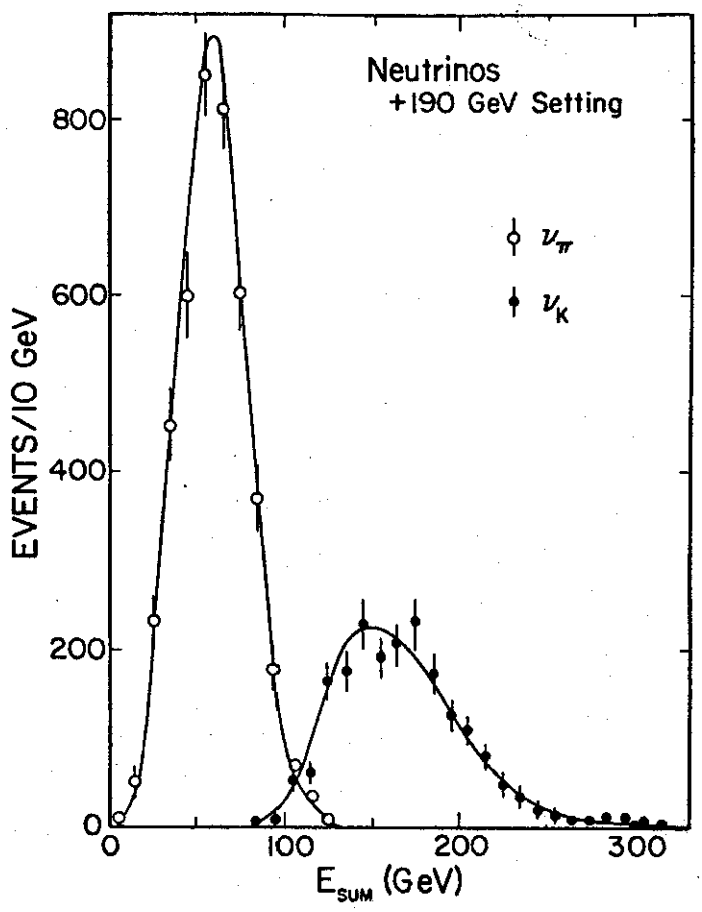

Fig. 3 Muon Trigger Events, selected as ν_π or ν_K, induced at the +190 GeV setting. The curves are the Monte Carlo predictions containing the experimental resolutions.

C. Separation of ν_π and ν_K Events (MT Events)

Figure 3 shows the distributions in the measured total energy at the beam setting of +190 GeV for the data in which all final state energy is measured; it is separated into events induced by pion neutrinos and kaon neutrinos. This separation was performed with an algorithm which incorporated the total measured energy as well as the location of the event in the target. The curves indicate the Monte Carlo prediction, which has our resolutions folded in. Mistakes in the separation of pion and kaon neutrino events would not be easily visible in this figure; the Monte Carlo calculation indicates that such errors are typically less than 2%. (The one exception to this is the $\bar{\nu}_\mu$ data induced by K^- at 130 GeV, where such errors may be as high as 8%. This has been taken into account in the error assignment.)

D. Azimuthal Acceptance Corrections (MT Events): Small y Cross-Sections

There are actually two sets of requirements (triggers) that could result in the data being recorded. For the moment, we will concentrate on one sample, called the muon trigger (MT) data, which has both the muon and the hadron energy measured on an event-by-event basis. (These data were obtained on the basis of a muon penetrating through the toridal analyzing magnet.) Because each event has all the final-state energy measured, the originating neutrino type for each event (ν_π or ν_K) is known (see Fig. 3).

All of the data you will see has been completely corrected for azimuthal losses. This correction involves rotating each individual event about the beam direction through 2π radians to determine the azimuthal fraction which would not trigger. This is often a rather substantial correction; it can account for as much as 80% of the acceptance losses. Using the events themselves to make the correction increases the statistical error, but has the comforting virtue that it is done in a manner that is independent of physics (unless one assumes that cross-sections depend on azimuthal angle). There are, of course, data at large polar angles (θ > 100mrad) which are not represented adequately in the MT sample.

At this stage, let us pause to see the MT data as represented in normalized y-distributions. I caution that, because this data has a finite polar angle cut-off ($\theta_1 \approx$ 100mrad), there are large remaining acceptance corrections, but these exist primarily at large y. Figure 4 shows as an example, the differential cross-section as a function of y for the kaon neutrino and antineutrino events at the ±190 GeV settings. The polar angle cut-off, θ_1, makes a cut-off in x as a function of y: $x_c y/(1-y) = E\theta_1^2/2M$, where M=nucleon mass. In this case there is full acceptance over x for $y \leqslant 0.45$. However, for lower neutrino energies, acceptance may become biased for y-values as low as 0.2. Additional data is required to quote total cross-sections; we will return to this point later.

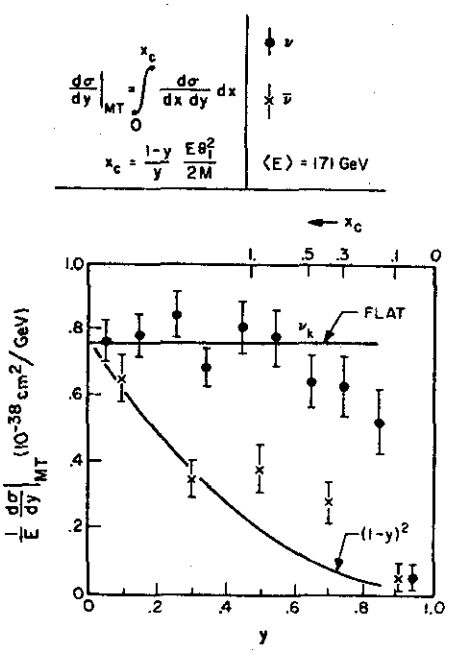

Fig. 4 Normalized differential cross-section vs. y for azimuthally corrected MT events. The flat and $(1-y)^2$ curves are drawn to guide the eye. The effect of the θ_1 = 100mrad cut-off on muon angle is visible at larger y($y \geqslant .45$). The flat $\bar{\nu}$ component, visible at larger y values, is substantially smaller than that seen in ν_μ.

Two important points which can be verified in the typical case of Fig. 4 are (1) the ν_μ and $\bar{\nu}_\mu$ data intercept the same point at y=0; and (2) there is a dramatic difference between neutrinos and antineutrinos at larger y, although there is clearly some flat component in $\bar{\nu}_\mu$. (The curves are only to guide the eye.) You might also notice that in the neutrino data there is no indication of a large upturn near y=0. In the CDHSB data presented at this conference, there seems to be a dramatic rise in the differential cross-section near y=0. I think this is sometimes referred to as the CERN high-rise.

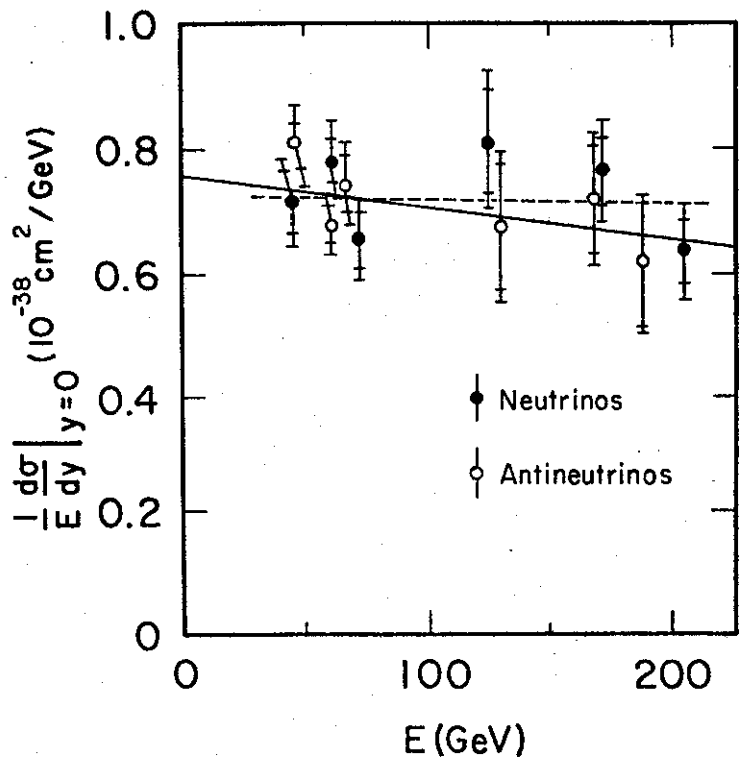

Fig. 5 Normalized y=0 cross-section for ν_μ and $\bar{\nu}_\mu$. The best two (solid line) and one (dotted line) parameter fits are shown. There is no evidence for substantial energy dependence or for $\nu,\bar{\nu}$ differences. The average of all points gives $\frac{1}{E}\frac{d\sigma}{dy}\Big|_{y=0} = (0.719 \pm 0.035) \times 10^{-38}\ \mathrm{cm}^2/\mathrm{GeV}$.

To further explore point (1) above, we present Fig. 5 to summarize the small y data for all of the beam settings. It shows the value of $d\sigma/dy$ at y=0, normalized by the neutrino energy, E. If charge symmetry is valid, ν_μ and $\bar{\nu}_\mu$ should give the same y-intercept at fixed E. Furthermore, if scaling is valid at low y, it should be independent of E. The plotted values in Fig. 5 are obtained by using events with $y < 0.2$, with a small correction for the extrapolation to y=0. We find no systematic

difference between neutrinos and antineutrinos at y=0 and we find no demonstrable energy dependence. The best fit allowing for some energy dependence is shown as the solid line; the best one parameter fit is shown as a dotted line. We believe that the y=0 equality of neutrino and antineutrino cross-sections has been demonstrated. If you already believed in charge symmetry at y=0, this equality demonstrates the correctness of our flux measurements.

Referring to the theoretical functional form of equation (1), you will observe that the differential cross-section at y=0 depends only on f_2. The value of $f_2 = \int F_2(x)dx$, extracted from the one parameter fit, is $f_2 = 0.46 \pm 0.02$, including the 4% overall normalization error. This compares quite favorably with the value of f_2 obtained from GGM total cross-section data(3) ($f_2 = 0.47 \pm .05$), in a similar range of Q^2 and ν values.

E. Azimuthal Acceptance Correction (HT Events): Total Cross-Sections

For accurate measurements of total cross-sections, the MT events are inadequate in polar angle acceptance. To supplement that data, we utilize events obtained (triggered) on the basis of a minimum deposition of hadron energy (HT events). These events do not necessarily have the muon energy measured, but each event is characterized by measured hadron energy and measured muon angle. (In fact, many events are triggered by both requirements. This redundancy is useful for making an experimental determination of the triggering efficiency for each.) The only requirement made of the muon in the HT event sample is that it be recognized as such. That is, it must penetrate past the hadron shower while still in the steel apparatus far enough to be recognized. Again, an azimuthal correction was made from the events themselves; acceptance in polar angle for this sample is good for $\theta \leqslant 360$mrad.

The separation of the total numbers of events in the ν_π and ν_K event samples is illustrated in Fig. 6 for the +190 GeV data sample. All azimuthally corrected HT events are plotted versus the measured hadron energy (E_h^m). In addition, the ν_K events from the MT trigger are plotted for $E_h^m < 90$ GeV, and the sum of ν_π and ν_K events are plotted for $E_h^m < 15$ GeV. (In these regions of y, the MT events cover the entire kinematic phase space.) Because the pion neutrino events are so much lower in energy, they cannot contribute to the HT events with $E_h^m > 90$ GeV. Therefore, the area indicated by ν_K represents the integrated ν_K signal; the cross-hatched area, obtained by subtracting the much smaller ν_K integral from the total, represents the total ν_π signal. Potential errors in this procedure, due to "leakage" of events from one regime to the other, have been investigated in detail and are typically very small.

This technique provides the separated totals of events induced by pion and kaon neutrinos at each beam setting, for polar angles $\theta < 360$mrad. This range of angles is quite appropriate for measurement of the total cross-section (see section F). I should also point out that this technique also results in the distributions in measured hadron energy, E_h^m, for the ν_π and ν_K fluxes separately. The means of these distributions give direct measures of mean y: $\langle y \rangle = \langle E_h^m \rangle / \langle E \rangle$. This relation

requires no corrections due to resolutions from either hadron energy, E_h, or neutrino energy, E. It does depend on self-consistent calibration of hadron energy and neutrino energy, which has been discussed.

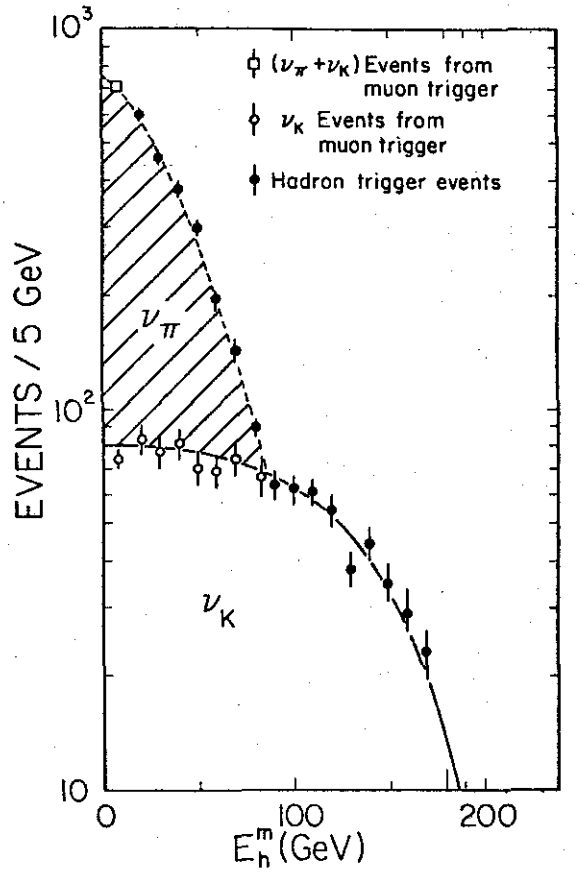

Fig. 6 Hadron energy distribution of azimuthally-corrected events from the MT and HT samples for neutrino running at the +190 GeV setting. The MT events, which are separated individually into ν_π and ν_K events by measurement, complete the pion and kaon samples at lower energies where the HT events are incomplete or ambiguous, respectively. Note that the ordinate is a logarithmic scale. The curves are drawn to guide the eye.

F. Corrections for Polar Angle Losses (θ_μ > 360mrads)

There remains a small loss of events due to requiring a penetrating muon in the HT sample. This loss was estimated by extrapolating the distribution in the scaled muon angle variable, $\kappa = 2M/E\theta^2$, to κ=0. In the worst case, this correction was 6.7% (lowest ν_π energy)

and typically it was of order 2%. We have incorporated a contribution to the total error that reflects our uncertainty on this correction. We believe that our corrected results represent true total cross-sections within the quoted uncertainty.

III. TOTAL CROSS-SECTIONS AND MEAN Y

The total cross-sections and mean y, integrated over all x, are shown in Fig. 7 as a function of the mean incident neutrino energy, E. Exact scaling would imply that σ/E and <y> are independent of energy. I wish to point out in passing that most of the error bar that is visible in Fig. 7 comes from the estimated systematic errors, although the statistical errors are certainly included.

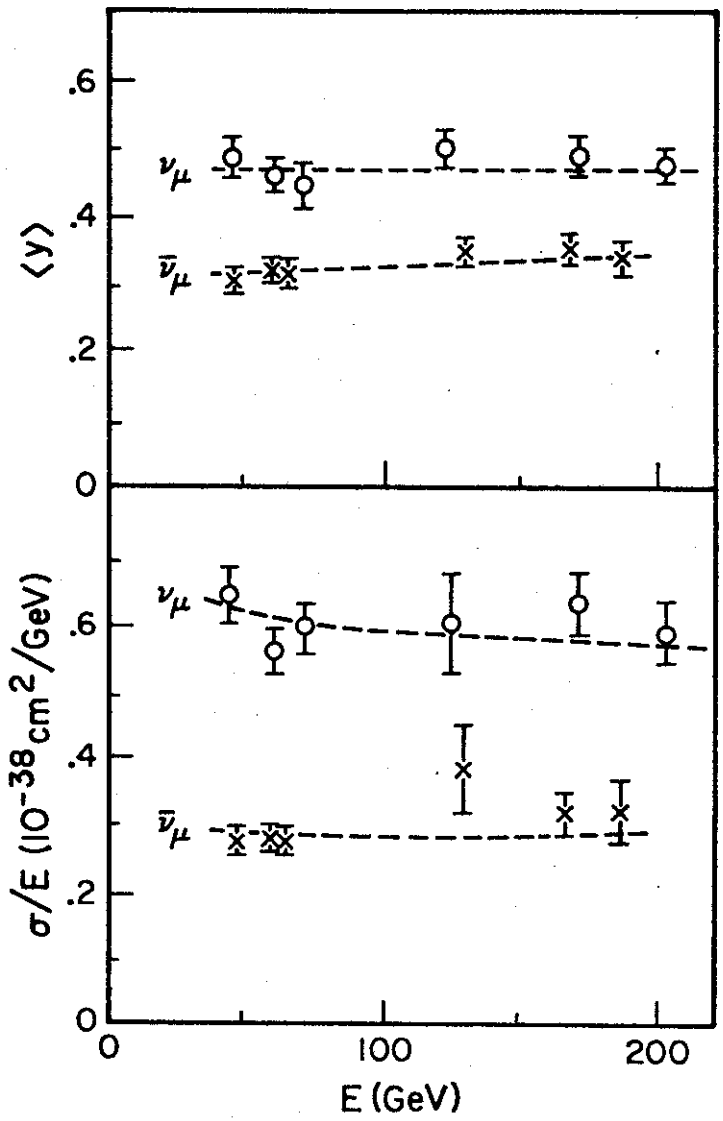

Fig. 7 The data from this experiment on <y> and σ/E for ν_μ and $\bar{\nu}_\mu$. The curves come from the best fit to the non-scaling 4-quark model described in the text. They give χ^2 = 14.1 for 22df.

A. Comparison with GIM (4 quarks) and Asymptotic Freedom

One question one might ask: how consistent is this data with simple theoretical ideas? That is, does it compare favorably with predictions based on putting in everything that one thinks must exist in neutrino physics without inventing new thresholds? The answer is that the data is not spectacularly different from that expected.[13] I have calculated the curves shown in Fig. 7 from a very simple 4-quark model, including charm, and including the effects of scale breaking as parameterized from the E-26 μp scattering data[14] at Fermilab. Allow me to refer to this as the GIM fit. Two parameters are left free: an overall normalization coefficient (g), and a coefficient (λ) proportional to the amount of strange quark in the ocean of $q\bar{q}$ that would make charmed final states. This latter parameter is defined such that λ=1 corresponds to an SU3 symmetric sea. The forms and integrals of the x-distributions were taken from fits[15] to the GGM and SLAC lepton scattering data. The slow-rescaling technique of Georgi and Politzer[16,17] was used to parameterize charm threshold. The curves fit the data quite well on the average, and even reproduce, without renormalizing the x-distributions ($g = 1.024 \pm .026$), the neutrino slope parameter (typically 0.61×10^{-38} cm^2/GeV in this data), which is much smaller than that measured in the GGM energy region (~0.74). Also, the best value of the strange component of the nucleon that comes from this fit is not unphysical ($\lambda = 0.55 \pm 0.17$). You might also notice, however, that the best fit predicts antineutrino cross-section and mean y-values which do not show quite as much energy dependence as the data points. I will return to this point later.

B. The b-Quark Hypothesis

One question that this data can address is the so-called b-quark hypothesis.[17] This would invent, in addition to what we have just discussed, new quarks with right-handed coupling to u quarks and coupling strength equal to the ud coupling. As you can see from Figs. 8a and 8b, this hypothesis does not fit the data well for b-quark masses less than 9 GeV. The data certainly do not require such additional quarks. This conclusion[13] is valid whether one puts scale breaking into the fits or not (see Fig. 8b). I think that no matter how one varies the detailed assumptions, one would rule out such quarks with masses of 8 GeV or lower. Of course, less massive quarks with a much smaller or very different (e.g. left-handed) coupling cannot be ruled out from this argument.

C. Comparison with HPWF Data[4]

One might also ask - how does this data compare with the previously published HPWF raw data [4] which has been interpreted to show substantial energy dependence in the cross-section ratio and mean y. Fig. 9a shows the cross-section ratio versus neutrino energy with the best GIM fit drawn through the points. The HPWF data, with relative normalization obtained in two ways, existed only in the lower part of the energy range. As you can see, the trend of the new data is very different. The same comment applies to Figure 9c: mean y for antineutrinos. I would like to reiterate that the CITFR data presented here

represent complete cross-sections, whereas the HPWF data being compared have complicated cuts at large x and in the quasi-elastic region. Therefore, the comparisons are not completely fair. However, since there has been some speculation regarding threshold behavior in this energy region, it is useful to compare the trend up to 200 GeV observed in the new, more complete data.

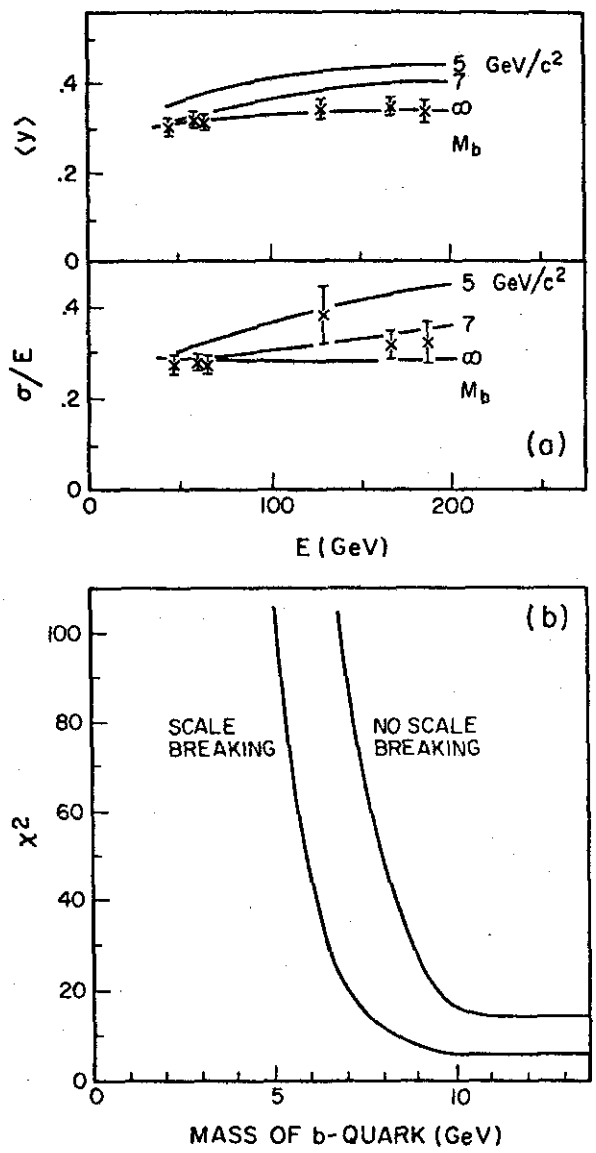

Fig. 8 (a) Scale-breaking fits to the anti-neutrino data with the inclusion of b-quark of the stated mass.
(b) χ^2 for fits to $\bar{\nu}$ data with and without scale breaking assumptions. There are 11 df. Under any assumptions, the usual b-quark mass must be greater than 8 GeV/c^2.

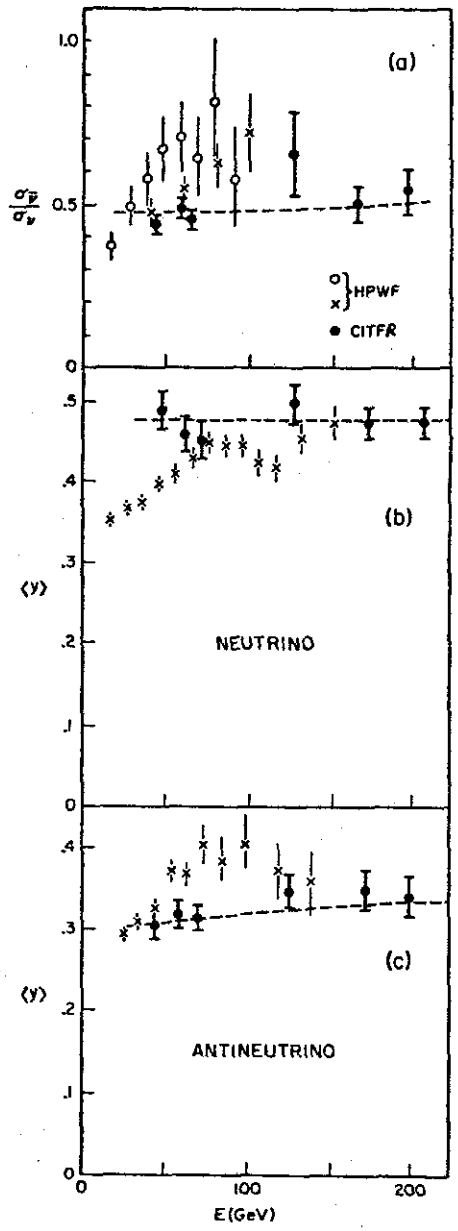

Fig. 9 Comparison of HPWF data with the results of this experiment. The two sets of data shown for the HPWF cross-section ratio use different techniques for flux normalization. The CITFR data include the entire kinematic range, while the HPWF data are cut at large x and in the quasi-elastic region.

D. The Question of Energy Dependence

Even though the CITFR data do not show the dramatic threshold behavior expected in some models, I think that it is a legitimate question to ask - is there any unexpected energy dependence at all? This can be a very important question. For example, there may be evidence,[18] from $\mu\mu$ production by protons, of a higher mass quark.[19] (No unexplained energy dependence by neutrinos would mean little coupling to such a quark.) Under these or any circumstances, the question of energy dependence is an important one, so we will ask it. Tables I and II attempt to address it by displaying the average of the low energy (ν_π) points and comparing to the average of the high energy (ν_K) points. In Table I (neutrinos), we see no indication of substantial difference at either small y, for the total cross-section, or for mean y. The conclusion follows that there is no evident energy dependence in these neutrino measurements over the range $45 < E < 205$ GeV. However, I would like to state again that the slope parameter, given in the second entry, is $0.61 \times 10^{-38} cm^2/GeV$, whereas the Gargamelle slope, measured at 5 GeV, is $0.74 \times 10^{-38} cm^2/GeV$. That difference (of many standard deviations) represents a 20% drop between 5 and 50 GeV. So, although the upper range alone shows no energy dependence, the comparison of the two results make it appear that all of the action is taking place below 50 GeV. It will be very useful to see accurate data in that energy range.

Table I

	E(GeV)	Neutrino Quantity	Value	Fractional Change $\frac{(K)-(\pi)}{\pi}$
(π)	58	$\frac{1}{E}\frac{d\sigma}{dy}\Big\|_{y=0}$	.720±.038	0.0±.086
(K)	164	in $10^{-38} cm^2/GeV$	.720±.049	
(π)	58	$\frac{1}{E}\sigma_{tot}$	.606±.021	+.031±.061
(K)	164	in $10^{-38} cm^2/GeV$	.618±.030	
(π)	58	<y>	.465±.014	+.034±.039
(K)	164		.481±.013	

For the antineutrinos in Table II, a different situation seems to prevail. As with neutrinos, we see no evidence for energy dependence near y=0. For the total cross-section, however, the weighted averages show about a 20% increase in the slope between 58 and 164 GeV; this is nominally a 3.4 standard deviation effect. Now, we can worry about the strength of that statement in a number of ways. (For example, the antineutrino point at 130 GeV, that seemed anomalous in Section IIB, can be dropped.) No matter how much reservation one applies, there is always an effect that is at least 2 standard deviations in the difference between low and high energies. Similarly, the averages of the mean y values for the low and high energies differ by about 11%, which is also a 2 standard deviation effect. (The value of the slope at 58 GeV is very similar to that of Gargamelle, which is also 0.28 cm^2/GeV.) This 2 standard deviation rise in $\frac{\sigma_{tot}}{E}$ and mean y between 58 and 164 GeV, while it is not of the magnitude that was predicted on the basis of b-quark (right-handed) models, is also not simply explained by asymptotic freedom effects and/or charm production. Additional measurements are needed to verify and explore the origin of this rise.

Table II

	E(GeV)	Antineutrino Quantity	Antineutrino Value	Fractional Change $\frac{(K)-(\pi)}{\pi}$
(π)	58	$\frac{1}{E}\frac{d\sigma}{dy}\Big\|_{y=0}$	.730±.034	-.082±.115
(K)	164		.670±.064	
(π)	58	$\frac{1}{E}\sigma_{tot}$	.282±.009	+.212±.063
(K)	164		.342±.025	
(π)	58	<y>	.311±.009	+.109±.042
(K)	164		.345±.018	

IV. Integrated Structure Functions

In the short time remaining, I would like to go quickly through this last question. For years, we have been using equation (1), together with the Callan-Gross relation, to extract values of the integrated structure functions. That procedure can also be applied here. However, with some indications that there are energy dependent effects, how appropriate is it to use this equation? If the energy dependence is slow enough, it may be that equation (1) remains a reasonable approximation at fixed neutrino energy, E.

For the first time, we have simultaneously determined experimental values for the first two moments of this differential cross-section, as well as the y=0 intercepts. This provides an overconstrained set of numbers, so that we can make sure that there are no large internal inconsistencies involved in the extraction of the structure functions.

A. Checking the Applicability of Equation (1)

If we assume the Callan-Gross relation ($f_1=f_2$) then the first two moments of equation (1) are:

$$\sigma^{\nu,\bar{\nu}} = \frac{G^2ME}{\pi} \{ \frac{2}{3} f_2 \pm \frac{1}{3} f_3 \} \tag{2}$$

$$\sigma^{\nu,\bar{\nu}}\langle y\rangle^{\nu,\bar{\nu}} = \frac{G^2ME}{\pi} \{ \frac{7}{24} f_2 \pm \frac{5}{24} f_3 \} \tag{3}$$

The zeroth moment is just the total cross-section, while the first moment is the product of cross-section and mean y. At fixed neutrino energy, we have four measurements: σ^{ν}, $\sigma^{\bar{\nu}}$, $\langle y\rangle^{\nu}$, and $\langle y\rangle^{\bar{\nu}}$, with only two unknowns: f_2 and f_3. The overconstraint is displayed by calculating the experimental values for the following ratios:

$$r_- = \frac{\sigma^{\nu}\langle y\rangle^{\nu} - \sigma^{\bar{\nu}}\langle y\rangle^{\bar{\nu}}}{\sigma^{\nu} - \sigma^{\bar{\nu}}} = \frac{\frac{10}{24} f_3}{\frac{2}{3} f_3} = \frac{5}{8} \tag{4}$$

and

$$r_+ = \frac{\sigma^{\nu}\langle y\rangle^{\nu} + \sigma^{\nu}\langle y\rangle^{\bar{\nu}}}{\sigma^{\nu} + \sigma^{\bar{\nu}}} = \frac{\frac{7}{12} f_2}{\frac{4}{3} f_2} = \frac{7}{16} \tag{5}$$

Deviations from these numbers would mean that the structure functions calculated from the 2 moments do not agree. Figure 10a shows the experimental values compared to the predicted number. No systematic difference is apparent, and the best average of the six points: 0.605 ± .026, is consistent with the predicted value of 5/8 = 0.625.

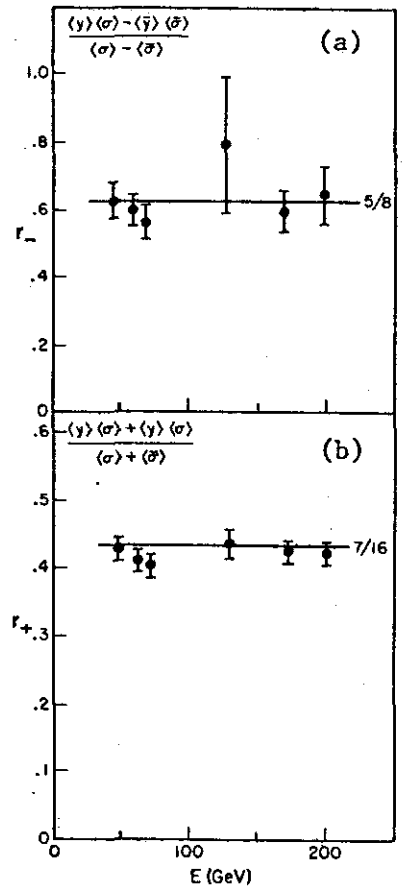

Fig. 10 Ratios of (a) differences and (b) sums of the cross-section moments compared to that predicted by equation (1).

Figure 10b shows the comparison of the data with Equation (5). The individual points lie close to the prediction. However, the overall average of the data: 0.424 ± .007, is more than a standard deviation from the prediction: 7/16 = 0.4375. This small difference (3%) could come from a variety of possible effects: e.g., a small difference between the f_3 of ν_μ and $\bar{\nu}_\mu$, or a small violation of the Callen-Gross relation. If, for example, we were to attribute the entire effect to the latter, we would obtain $(f_2 - f_1)/f_2 = +0.17 \pm 0.09$. We conclude, however, that the structure functions determined by the data are self-consistent at the 3% level.

B. Structure Functions Versus Energy

Using all of the data to obtain f_2 and f_3 from Equations (2) and (3), we plot these valued in Fig. 11a and 11b. (The error bars shown do not have the 4% overall systematic error folded in, since for the most part the comparisons being made are internal to this data set.) The integrated value f_3, shown in Fig. 11a, indicates some energy dependence, especially when compared to the low energy GGM point.[3] By contrast, the values of f_2 show no strong indication of energy dependence. The best average of the six points is $\langle f_2 \rangle = 0.430 \pm 0.008$. This value is slightly lower than, for example, that extracted from the small-y data: $f_2 = 0.455 \pm 0.013$.

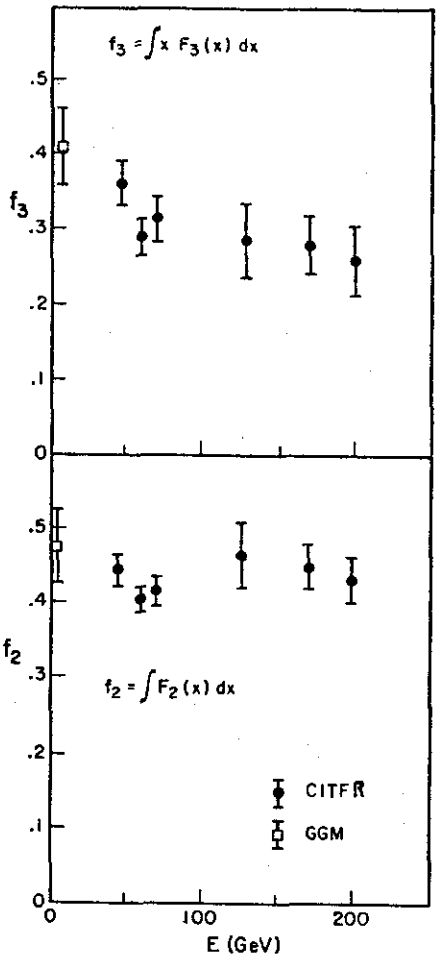

Fig. 11 Values of the integrated structure functions from this experiment compared with the lower energy GGM point.(3)

This small difference could come about from either some Q^2 or energy dependence (non-scaling) in $F_2(x)$, or from a Callan-Gross violation at the level of 17%. Fig. 1, shown in the beginning of the talk, gives the ratios of the values in Fig. 11. One must conclude that the energy dependence indicated in the $\sigma^{\bar{\nu}}$ and $\langle y \rangle^{\bar{\nu}}$ values is more likely to come from energy dependence in F_3 than from energy dependence in F_2.

V. CONCLUSIONS

This data permits the following specific conclusions to be drawn:

(1) The test of charge symmetry at low energy transfers

$$\left.\frac{d\sigma^{\nu}}{dy}\right|_{y=0} = \left.\frac{d\sigma^{\bar{\nu}}}{dy}\right|_{y=0}$$

is valid at the 5% level. There is no observable energy dependence over the energy range of this experiment.

(2) The values of σ/E and $\langle y \rangle$ for neutrinos show no obvious energy dependence over the range $45 < E < 205$ GeV. However, the slope parameter, σ/E, is lower than the GGM value by about 20%. This encourages some effort in the energy range $E < 45$ GeV to delineate the physical origin of this difference.

(3) The value of σ/E for antineutrinos at 58 GeV is similar to the GGM value[3] measured at much lower energy. However, there is a two standard deviation rise between 58 and 164 GeV in both σ/E (~20%) and $\langle y \rangle$ (~10%).

(4) This data does <u>not</u> substantiate the <u>dramatic</u> rise in $\sigma^{\bar{\nu}}/\sigma^{\nu}$ or $\langle y \rangle^{\bar{\nu}}$, that was indicated by the HPWF data.[4]

(5) Right-handed quarks[16] coupled through the Fermi constant to u-quarks are ruled out in the mass range $M_b \lesssim 8$ GeV.

(6) Some qualitative features of the data may find explanation in the scale-breaking effects[13] seen in μp and ep scattering. This is particularly true for the magnitudes of $\langle y \rangle$ and σ/E measured with neutrinos.

(7) The data are not in serious disagreement with the form of the standard Equation (1) at fixed E. The small deviations indicated by Fig. 10 may find explanation in scale-breaking effects, small charge-asymmetric effects, and/or violations of the Callan-Gross relation. The 2 SD energy-dependent effects in the antineutrino data are more likely to come from energy dependence of the F_3 structure function than the F_2 structure function.

REFERENCES

(1) See, e.g. C. H. Llewellyn-Smith, Physics Report 36, 623 (1972).

(2) G. Myatt and D. H. Perkins, Phys. Lett. 34B, 542 (1971).

(3) T. Eichten et al., Phys. Lett. 46B, 274 (1973); W. G. Scott, Ph.D. Thesis, University of Oxford (December 1974).

(4) B. Aubert et al., Phys. Rev. Lett. 33, 984 (1974);
A. Benvenuti et al., Phys. Rev. Lett. 36, 1478 (1976);
A. Benvenuti et al., Phys. Rev. Lett. 37, 189 (1976).

(5) B. C. Barish et al., Phys. Rev. Lett. 38, 314 (1977).

(6) B. C. Barish et al., Phys. Rev. Lett. 35, 1316 (1975).

(7) J. P. Berge et al., Proceedings of the International Neutrino Conference, Aachen 1976 (presented by F. A. Nezrick), pg. 362.

(8) B. C. Barish et al., Phys. Rev. Lett. 39, 741 (1977).

(9) B. C. Barish et al., CALT 68-611 (to be submitted for publication).

(10) B. C. Barish et al., CALT 68-605 (submitted for publication).

(11) B. C. Barish et al., CALT 68-606 (to be submitted for publication).

(12) B. C. Barish et al., Phys. Rev. Lett. 39, 981 (1977).

(13) Qualitatively similar conclusions have been drawn by others. See e.g. R. M. Barnett, SLAC-PUB-1961 (June 1977) and G. C. Fox CALT-68-619 (Sept. 1977).

(14) Y. Watanabe et al., Phys. Rev. Lett. 35, 898 (1975); C. Chang et al., Phys. Rev. Lett. 35, 901 (1975).

(15) W. J. Wilson, LBL-3862 (June 1975).

(16) H. Georgi and H. D. Politzer, PR D14, 1829 (1976).

(17) R. M. Barnett, PRL 36, 1163 (1976) and PR D14, 70 (1976).

(18) S. W. Herb et al., PRL 39, 252 (1977).

(19) See, e.g., C. E. Carlson and R. Suaya, PRL 39, 908 (1977).

DISCUSSION PERIOD

Tong (MIT): When you obtained the integrals over the structure functions, did you explain how you correct for the x-regions where you have poor acceptance?

Sciulli: We measure the normalized cross-section for charged-current events with secondary muons of polar angle $\theta < \theta_1 = 360$ mrad. (This cut is necessary so that we will not be contaminated by neutral current events.) This means that there is a finite region of phase space, at rather large x and y, which is not completely covered $\frac{xy}{1-y} > \frac{E\theta_1^2}{2M}$. The correction for this loss is, however, small. The distribution shown in the figure is at the energy setting for which the worst loss occurs, pion neutrinos with $\langle E \rangle = 45$ GeV. The abscissa is the scaled muon angle: $K_\theta = 2M/E\theta^2$. As you see, the missing events lie totally within the lowest bin. By extrapolating the distribution to zero, we obtain an estimate of 235 events to be added to the 3500 observed events, or a 6.7% correction. At the higher neutrino energies, the correction becomes smaller; at the highest energies it is less than a percent. For anti-neutrinos, with fewer events at large y, the corresponding distribution is essentially flat, and the correction is always less than 2%.

Cline: Would you explain why you have not shown an x-distribution and whether you think you can measure it?

Sciulli: As you may have noticed, the way we have done the experiment is to utilize the properties of the narrow band beam so that we could incorporate events in which the muon energy was not measured. This has permitted us to measure σ_{tot} and $\langle y \rangle$ for the complete sample of events at fixed energy. However, in order to measure x with reasonable resolution for individual events, we must use only events in which the muon energy was measured. This subsample has very poor acceptance at larger y. At the same time, events at small y have very poor resolution for determination of x, as you know. Therefore, I believe that measurements of the details of x-distributions in this data could not be conclusive. Our new experiment, with improved acceptance at large x and y should be substantially better in this regard.

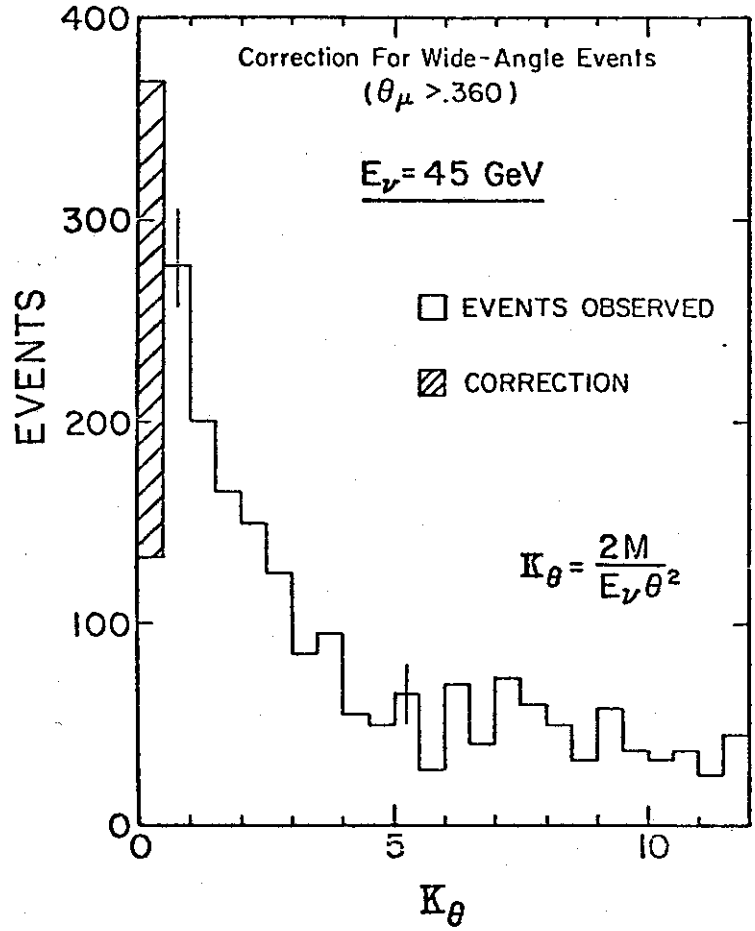
Correction For Wide-Angle Events
(θ_μ >.360)
E_ν= 45 GeV
EVENTS OBSERVED
CORRECTION
$K_\theta = \frac{2M}{E_\nu \theta^2}$
EVENTS
400
300
200
100
0
0
5
10
K_θ